Journal of Molecular Spectroscopy 403 (2024) 111926

Contents lists available at ScienceDirect

Journal of Molecular Spectroscopy

journal homepage: www.elsevier.com/locate/yjmsp

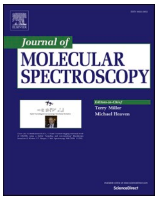

Microwave spectra of two carboxylic acid anhydrides: Acetic anhydride and acetic difluoroacetic anhydride

Nathan Love, Kenneth J. Koziol, Kaitlyn Belmont, Kenneth R. Leopold *

Department of Chemistry, University of Minnesota, 207 Pleasant St., SE, Minneapolis, MN 55455, United States

A R T I C L E I N F O

Keywords:
Acetic anhydride
Acetic difluoroacetic anhydride
Microwave spectrum
Conformation

A B S T R A C T

Microwave spectra of acetic anhydride, D6-acetic anhydride, and acetic difluoroacetic anhydride have been observed in a supersonic jet. In conjunction with accompanying DFT and MP2 calculations, these systems are shown to adopt a nonplanar configuration in which the C=O groups point in approximately orthogonal directions. Methyl group internal rotation was fully analyzed for both species. The observed conformation of these systems appears to result from an interaction between a CH_3 hydrogen (in acetic anhydride) or the CF_2H hydrogen (in acetic difluoroacetic anhydride) with the carbonyl group to which it is not directly bound, forming a six-membered ring. The fitted rotational constants for both systems are in reasonably good agreement with calculated values, but for acetic anhydride, the agreement is somewhat worse than that previously observed for a series of *syn* anhydrides. The calculations indicate a pronounced flexing of the heavy atom frame as the CH_3 group in the six-membered ring undergoes internal rotation, and this likely influences the level of agreement between the theoretical and vibrationally averaged experimental constants. The other CH_3 group does not interact with a carbonyl oxygen because of its orientation in the molecule, and its internal rotation does not induce similar changes in the molecular frame. In the acetic difluoroacetic anhydride, it is the CF_2H hydrogen that interacts with its remote carbonyl oxygen, leaving the internally rotating CH_3 group unaffected by participation in a six-membered ring and giving rise to much smaller deviations in the rotational constants as it moves along its internal rotation coordinate. Correspondingly better agreement between experimental and theoretical spectroscopic constants is obtained.

1. Introduction

Recent work in our laboratory has examined the conformation of several carboxylic acid anhydrides [1–3], i.e., RCOOCOR', with (R,R') = (CH_3, CF_3), ($C(CH_3)_3$, CF_3), (C_6H_5, CF_3), (CH_3, $C(CH_3)_3$), ($(CH_3)_3$, $(CH_3)_3$) and (CF_3, CF_3). Both microwave spectra and accompanying M06-2X/6-311++G(d,p) and MP2/6-311++G(d,p) calculations established that these systems adopt a *syn* conformation (roughly described as "nonplanar *cis*" in that work). In this configuration, the two carbonyl groups are pointed in approximately the same direction, but are twisted out of plane so as to produce a non-zero O=C···C=O dihedral angle. This angle varied depending on the nature of the R groups, and was observed to correlate with the average of the O=C stretching frequencies of the parent acids. Consistent with the computational results, the observation of the *syn* conformers under supersonic expansion conditions indicated that these are, indeed, the lowest energy forms. In most cases, higher energy, nonplanar *t-gauche* conformers were also predicted computationally, but none were observed. Only for (R, R') = (CH_3, $(CH_3)_3$) was a nonplanar *t-gauche* form not identified on the potential energy surface by the theoretical methods employed [1]. (See below for the specific meaning of the "*t-gauche*" designation.)

The *syn* conformations are in sharp contrast with the reported structures for formic and formic acetic anhydrides. For formic anhydride, (R,R') = (H,H), gas phase electron diffraction [4,5], microwave [6,7], and infrared [5] experiments ultimately established a *trans planar* geometry. Formic acetic anhydride, (R,R') = (H, CH_3), has also been studied by electron diffraction [8,9], microwave [10], and infrared and Raman [9,11] techniques and confirmed to adopt a conformation in the gas phase that is best described as *trans* planar (ignoring the out-of-plane methyl hydrogens). Both of these species contain a formyl hydrogen and the planar arrangement has been attributed to the acidity of that hydrogen and its corresponding ability to form a hydrogen bond to the remote carbonyl oxygen (i.e., the oxygen of the carbonyl to which it is not directly attached) [9]. In other words, a hydrogen bond between the

---

* Corresponding author.
E-mail address: kleopold@umn.edu (K.R. Leopold).

https://doi.org/10.1016/j.jms.2024.111926
Received 26 March 2024; Received in revised form 20 May 2024; Accepted 14 June 2024

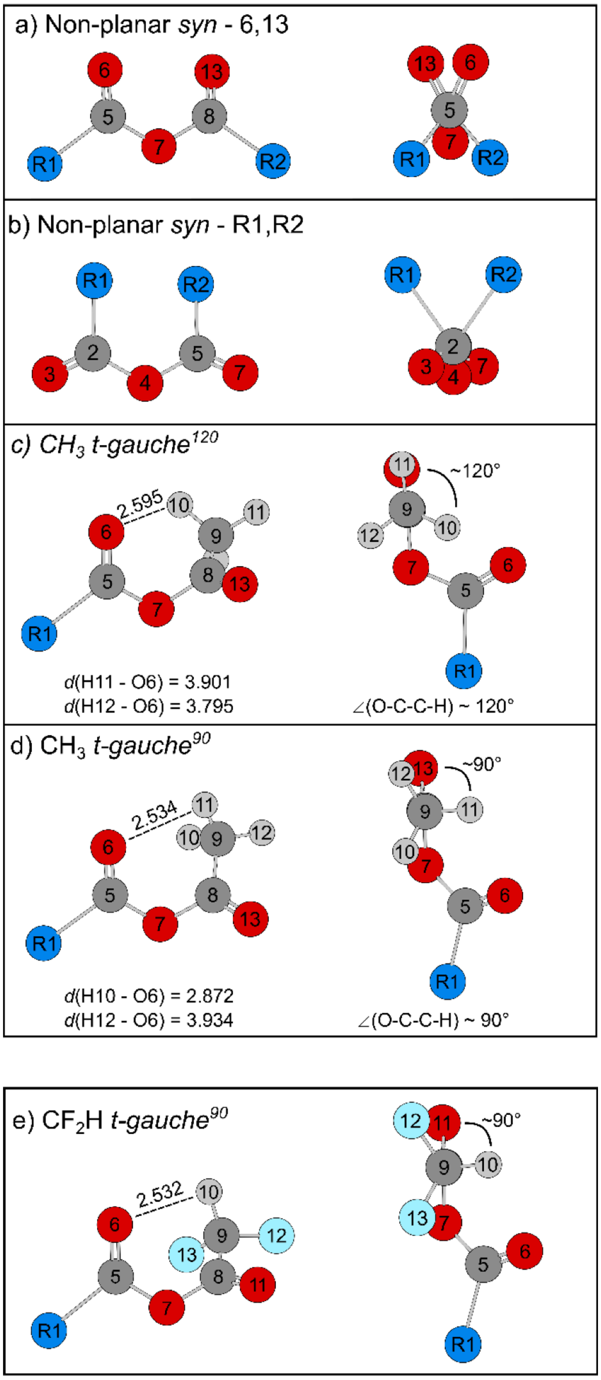

Fig. 1. Nonplanar carboxylic anhydride conformers predicted in this study. Note that the CF_2H *t-gauche*^{90} conformer is analogous to the CH_3 *t-gauche*^{90} conformer of acetic anhydride, but the difluoromethyl group is hydrogen bonded rather than the methyl group. The dashed lines highlight the internal hydrogen bonds in the *t-gauche* conformers. Views on the right side of each panel of the *t-gauche* conformers is viewed through the C—C bond of the O=C—C—H dihedral angle (H refers to the hydrogen bonded methyl hydrogen). The *syn*-6,13 in panel a indicates that O6 and O13 point in approximately the same direction whereas the *syn*-R1,R2 labels in panel b indicates that the methyl groups (R1 and R2) point in approximately the same direction.

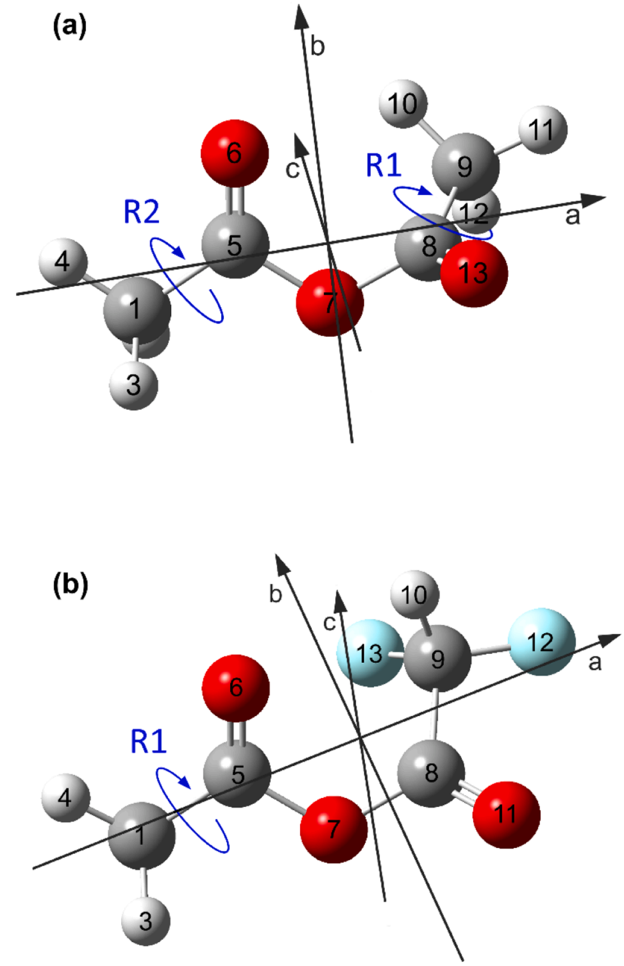

Fig. 2. (a) Optimized structure of acetic anhydride in *t-gauche* configuration calculated at the MP2/6–311++G(d,p) level of theory. R1 is labeled as the methyl rotor that interacts with the carbonyl group to which it is not attached, and R2 is the isolated methyl rotor at the periphery of the molecule. H2 is obstructed from view by C1 at this angle. (b) Optimized structure of acetic difluoroacetic anhydride calculated at the MP2/6–311++G(d,p) level of theory. H2 is again obstructed from view by C1 at this angle.

formyl hydrogen and the remote carbonyl oxygen is the likely energetic driver for the planar *trans* geometry.

In this paper, we present a microwave and computational study of acetic anhydride, (R,R') = (CH_3, CH_3), and acetic difluoroacetic anhydride, (R,R') = (CH_3, CF_2H). Neither of these species contains a formyl hydrogen, though the hydrogen on the CF_2H group in the latter should also have the ability to form a strong internal hydrogen bond to the remote carbonyl oxygen. Thus, both systems stand to provide interesting comparisons with the *syn* and planar *trans* conformations adopted by the other anhydrides noted above. Acetic anhydride has been studied by vibrational spectroscopy [12,13] and electron diffraction [12,14] but, to date, no microwave spectra have been reported. We are unaware of any previous spectroscopic or electron diffraction studies of acetic difluoroacetic anhydride. The infrared spectra and electron diffraction results for acetic anhydride (obtained at slightly elevated temperatures) were successfully analyzed by considering two conformers simultaneously [12]. As discussed below, we find a twisted *gauche*-like geometry for both species when observed under supersonic jet conditions. The observation of this form at the low temperature of the jet suggests that it is the lowest in energy, though higher energy, *syn* configurations are also predicted computationally.

2. Computational methods and results

Calculations were performed at the M06-2X/6-311++G(d,p) and MP2/6-311++G(d,p) levels of theory using Gaussian 16 [15]. These methods were chosen because, in our previous studies of carboxylic acid anhydrides [1–3], they gave good to excellent agreement between experimental and theoretical rotational constants and internal rotation parameters at the global potential energy minimum. Moreover, for pivalic [3] and pivalic trifluoroacetic anhydride [1], they accurately reproduced bond lengths and bond angles determined from extensive isotopic substitution within the heavy atom frame. As discussed below, both *syn* and twisted *gauche*-like structures were identified for both acetic and acetic difluoroacetic anhydride. All reported structures were checked for the absence of imaginary frequencies and zero-point corrected energies using harmonic frequencies were also calculated. In the discussion that follows, the term "twisted *gauche*-like" (abbreviated "*t-gauche*") is used to describe a configuration in which the O=C⋯C=O dihedral angle is in the range that would normally be described as "*gauche*". However, since the carbonyl groups are not adjacent (as would normally be the case for use of the term gauche) but are, instead, separated by a bridging oxygen atom, we refrain from simply using "*gauche*" to avoid any confusion that might otherwise be implied about the stereochemical configuration of the molecule as a whole.

2.1. Acetic anhydride

The M06-2X and MP2 methods predict two *syn* conformers for acetic anhydride. These are shown in Fig. 1a and 1b, where the "*syn*-6,13" notation refers to the structure in which O6 and O13 carbonyl groups point in approximately the same direction, while the *syn*-R1,R2 designation refers to the structure in which the two methyl groups point in approximately the same direction. The energy of the *syn*-R1,R2 form is 8.0 kcal/mol higher than that of the lowest energy structure and its calculated rotational constants (in MHz, at the MP2 level) are (*A, B, C*) = (4885, 1839, 1692), which are in very poor agreement with the experimentally determined values. Thus, while we acknowledge its existence as a local minimum on the potential energy surface by including it in Fig. 1, it is not considered any further in this work.

The potential energy landscape near the *t-gauche* configuration is somewhat more complex. The M06-2X calculations identified a single minimum, designated *t-gauche*^{90}, while the MP2 calculations found two minima, labeled *t-gauche*^{90} and *t-gauche*^{120}. This nomenclature derives from the approximate dihedral angle between the C8 = O13 bond and the C9-H10 bond (i.e. H10-C9-C8-O13), as illustrated in Fig. 1c and 1d. The O=C⋯C=O dihedral angles in the *t-gauche*^{90} and *t-gauche*^{120} configurations (i.e., the angle between the normal vectors to the O6-C5-O8 and C5-C8-O13 planes) are 109.0 and 84.7 degrees, respectively, as determined from the MP2 structures. The twisted *gauche*-like geometry is evident in Figs. 1 and 2. Energies are given in Tables 1 and 2, both with and without harmonic zero-point corrections, and the optimized geometry, with atom numbering, is shown in Fig. 2a. The figure also defines the two methyl rotors, R1 and R2. Tables of Cartesian coordinates are given in the Supplementary Material.

The difference between the *t-gauche*^{90} and *t-gauche*^{120} structures is subtle and moreover, the two *t-gauche* structures are only predicted at the MP2 level. This prompted a set of further calculations along the CH_3 internal rotation coordinate. Fig. 3 shows the calculated electronic energy obtained by both the M06-2X and MP2 methods as the methyl group rotates. The left panel displays the effect of rotation of R1 and the

Table 1

Fitted and Computed Spectroscopic Constants for Parent Acetic Anhydride and Comparison with Theoretical Results.

	Full Fit	$K_a = 0$ and 1 Fit	M06-2X[a]		MP2[a]		
			syn	CH_3 *t-gauche*^{90}	*syn*	CH_3 *t-gauche*^{90}	CH_3 *t-gauche*^{120}
A [MHz]	5253.5233(67)	5253.467(64)	5552	5350	5442	5261	5188
B [MHz]	1825.7247(32)	1825.83(12)	1811	1895	1801	1864	1800
C [MHz]	1642.5546(28)	1642.45(12)	1541	1535	1542	1573	1697
Δ_J [kHz]	1.860(35)	2.60(75)					
Δ_{JK} [kHz]	12.85(12)	9.3(47)					
Δ_K [kHz]	–12.82(55)	–73(57)					
δ_J [kHz]	–0.495(14)	–0.476(51)					
δ_K [kHz]	64.9(11)	119(57)					
F_0^{R1} [GHz]	[158.5][b]	[158.5][b]					
V_3^{R1} [cm^{-1}]	241.4(97)	238.9(74)	289	280	295	194	194
ε^{R1} [deg]	24.170(87)	24.056(43)	32	19	34	23	27
δ^{R1} [deg]	73.886(22)	73.957(14)	41	81	41	81	72
$D_{\pi 2J}^{R1}$ [MHz]	0.477(21)	0.488(16)					
$D_{\pi 2K}^{R1}$ [MHz]	–1.850(74)	–2.009(70)					
$D_{\pi 2-}^{R1}$ [MHz]	–2.348(69)	–2.394(84)					
F_0^{R2} [GHz]	[157.9][b]	[157.9][b]					
V_3^{R2} [cm^{-1}]	207.8(20)	208.0(12)	289	222	295	222	161
ε^{R2} [deg]	40.00(11)	40.167(53)	32	26	34	33	48
δ^{R2} [deg]	28.357(30)	28.333(17)	41	34	41	33	28
$D_{\pi 2J}^{R2}$ [MHz]	–0.0923(53)	–0.0882(25)					
$D_{\pi 2K}^{R2}$ [MHz]	–0.477(29)	–0.511(28)					
$D_{\pi 2-}^{R2}$ [MHz]	1.471(41)	1.559(33)					
V_{cc} [cm^{-1}]	21.4(16)	22.8(19)					
N[c]	258	153					
σ [kHz]	56.0	14.4					
$\lvert\mu_a\rvert$ [D]	Strong		0.0	2.0	0.0	1.7	1.2
$\lvert\mu_b\rvert$ [D]	Strong		4.0	0.7	3.6	0.7	0.9
$\lvert\mu_c\rvert$ [D]	Strong		0.0	1.9	0.0	2.2	2.8
Rel. Energy[b]	–		0.13 (–0.05)	0.00	0.00	0.77 (0.88)	0.66 (0.63)

(a) All energies are in kcal/mol and were obtained using the 6–311++G(d,p) basis set. Values in parentheses are zero-point corrected. Uncorrected energies are relative to the most stable conformer calculated at the same level of theory. Zero-point corrected energies are relative to the form that has the lowest zero-point corrected energy. In cases where *t-gauche*^{90} and *t-gauche*^{120} minima are predicted, the energy given is that of the lower energy structure. A negative sign indicates that the energy ordering of the conformers inverts after zero-point correction. Calculated rotational constants are equilibrium values.

(b) Theoretical value, constrained in fit.

(c) Number of transitions in the fit.

middle panel shows that of rotation of R2. It may be seen from Fig. 3a that, while the M06-2X calculations do not predict an energy minimum at the *t-gauche*^{120} structure, there is a clear inflection where the MP2 calculations do. This is similar to previously reported calculations on the "*trans*" conformations of acetic trifluoroacetic and acetic pivalic anhydrides [1]. (Note, however, that for those systems, the "*trans*" (or *t-gauche*) form is not the lowest energy conformer).

In light of the above, it is unclear whether this secondary minimum is real or, if it is, whether it is relevant to the vibrationally averaged structure. What the calculations show, however, is that in either *t-gauche* configuration, one of the methyl hydrogens (designated, here, the "bound" hydrogen) appears to be interacting with the remote carbonyl oxygen, forming a six-membered ring. Close examination further reveals that the two structures differ as to which methyl hydrogen is bound (see Fig. 1). Stated differently, as the methyl group rotates, one or the other of the hydrogens (H10 or H11) interacts with the remote carbonyl depending on the value of the internal rotation coordinate. This manifests as sudden change that is accompanied by an abrupt flexing of the heavy atom frame and it is distinct from the smooth interchange of the hydrogens that would normally accompany three-fold rotation of the methyl group. The switching of the bound vs. "unbound" hydrogen gives rise to either a secondary potential minimum or an inflection in the internal rotation profile, depending on the method of calculation. The internal rotation of R2 (central panel of Fig. 3) shows much more regular behavior, which is sensible as it is not near enough to its remote carbonyl for there to be an appreciable intramolecular interaction.

Accompanying the switching of the bound hydrogen and the flexing of the molecular frame is an abrupt change in the instantaneous rotational constants of the molecule. Fig. 4 presents plots of these changes as a function of the internal rotation coordinate. The blue trace corresponds to rotation of the methyl rotor involved in the six-membered ring (R1) and the red trace is that for the isolated methyl rotor (R2). Clearly, while internal rotation of the isolated methyl group produces some changes in the rotational constants, those changes are a smooth function of the internal rotation angle. In contrast, abrupt changes are seen upon internal rotation of R1 and correspond to an abrupt switching of the methyl hydrogen that interacts with the remote carbonyl, giving rise to an accompanying reconfiguration of the molecular frame. A video illustrating this effect is provided in the Supplementary Material.

As seen in Table 1, *syn* and *t-gauche* forms are nearly isoenergetic, with relative energies differing by less than 1 kcal/mol. At the levels of theory employed, these differences are too small to reliably draw conclusions as to which structure represents the global energy minimum. Thus, additional calculations at the M06-2X/6-311++G(d,p) and MP2/6-311++G(d,p) geometries were performed at the DLPNO-CCSD(T)/aug-cc-pVTZ and DLPNO-CCSD(T)/aug-cc-pVQZ levels of theory. These calculations also indicated very similar energies for the *syn* and *t-gauche* structures, with differences of only a few tenths of a kcal/mol. Thus, we conclude that the *syn* and *t-gauche* structures are so similar in energy that theory cannot establish their relative energy ordering. This conclusion is consistent with the experimental estimate of Wu et al. [12], which places the energy difference between the *syn* and *t-gauche* conformers (termed sp,sp and sp,ac in that work) at about 0.1 kcal/mol. The experiments described below, however, do enable the likely energy ordering to be established due to the ultra-cold (~2K) temperature of the supersonic jet. The CCSD results are included in the Supplementary Material.

2.2. *Acetic difluoroacetic anhydride*

Acetic difluoroacetic anhydride is simpler than acetic anhydride because it contains only one methyl rotor. However, there is the additional complication that either the CF_2H hydrogen or a CH_3 hydrogen can interact with its remote carbonyl to form a six-membered ring. This gives rise to the possibility of "CF_2H *t-gauche*" structure (Fig. 1e) or "CH_3 *t-gauche*" structure, the former being distinctly lower in energy

Table 2
Fitted and Computed Spectroscopic Constants for D6-Acetic Anhydride and Comparison with Theoretical Results.

	Full Fit	**$K_a = 0$ and 1 Fit**	**M06-2X**^{a}		**MP2**^{a}		
			syn	CH_3 *t-gauche*^{90}	*syn*	CH_3 *t-gauche*^{90}	CH_3 *t-gauche*^{120}
A [MHz]	4592.2901(27)	4592.300(11)	4892	4636	4807	4567	4555
B [MHz]	1599.8448(14)	1599.841(70)	1553	1668	1545	1640	1573
C [MHz]	1440.6333(14)	1440.636(68)	1337	1360	1337	1393	1482
Δ_J [kHz]	1.8348(98)	1.82(44)					
Δ_{JK} [kHz]	11.371(49)	11.2(28)					
Δ_K [kHz]	–11.64(19)	–					
δ_J [kHz]	–0.3121(59)	–0.317(42)					
δ_K [kHz]	66.76(43)	66(34)					
F_0^{R1} [GHz]	[79.44]^b	[79.44]					
V_3^{R1} [cm^{-1}]	184.99(11)	185.10(15)	289	280	295	194	194
ε^{R1} [deg]	18.27(83)	16.24(93)	32	19	34	23	27
δ^{R1} [deg]	70.583(52)	70.44(11)	41	81	41	81	72
F_0^{R2} [GHz]	[79.32]^b	[79.32]^b					
V_3^{R2} [cm^{-1}]	174.453(61)	174.541(73)	289	222	295	186	161
ε^{R2} [deg]	56.61(31)	55.68(68)	32	26	34	33	48
δ^{R2} [deg]	26.89(13)	26.96(16)	41	34	41	33	28
N^c	175	90					
σ [kHz]	14.3	12.3					
$\lvert\mu_a\rvert$ [D]	Strong		0.0	1.9	0.0	1.7	1.1
$\lvert\mu_b\rvert$ [D]	Strong		4.0	0.9	3.6	0.9	1.3
$\lvert\mu_c\rvert$ [D]	Strong		0.0	1.9	0.0	2.1	2.6
Relative Energy^b	–		0.13 (0.01)	0.00	0.00	0.77 (0.85)	0.66 (0.63)

(a) All energies are in kcal/mol and were obtained using the 6–311++G(d,p) basis set. Values in parentheses are zero-point corrected. Uncorrected energies are relative to the most stable conformer calculated at the same level of theory. Zero-point corrected energies are relative to the form that has the lowest zero-point corrected energy. In cases where *t-gauche*^{90} and *t-gauche*^{120} minima are predicted, the energy given is that of the lower energy structure. Calculated rotational constants are equilibrium values.

(b) Theoretical value, constrained in fit.

(c) Number of transitions in the fit.

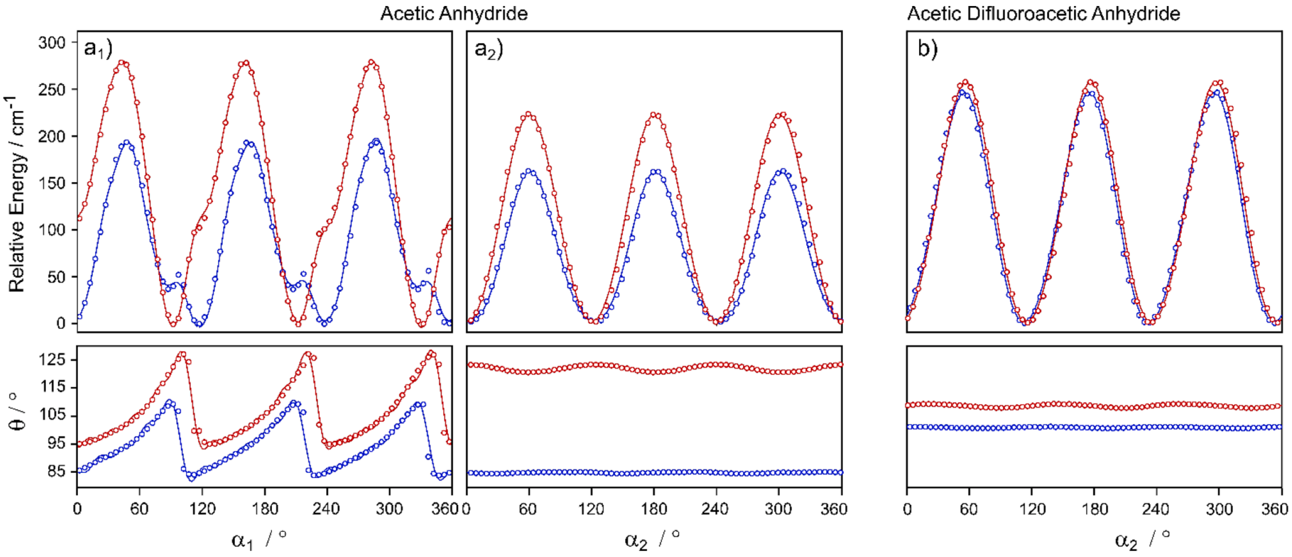

Fig. 3. Energy profiles of the methyl internal rotation in (a) acetic anhydride and (b) acetic difluoroacetic anhydride, calculated at the MP2/6-311++G(d,p) (blue) and M06-2X/6-311++G(d,p) (red) levels of theory. For acetic anhydride, the methyl group internal rotation angles are designated α_1 and α_2, corresponding to the rotors labeled in Fig. 1. For acetic difluoroacetic anhydride, the one methyl group is still labeled α_2 so that the notation consistently applies a subscript "2″ to the CH_3 group that does not interact with a remote carbonyl. Specifically, $\alpha_1 = \angle(H10\text{-}C9\text{-}C8\text{-}O13)$ and $\alpha_2 = \angle(\text{H2-C1-C5-O6})$. Energies are relative to the corresponding minima in each individual scan. θ is the through-space dihedral angle $\angle(\text{O6-C5-C8-O13})$ between the carbonyl groups. (For interpretation of the references to color in this figure legend, the reader is referred to the web version of this article.)

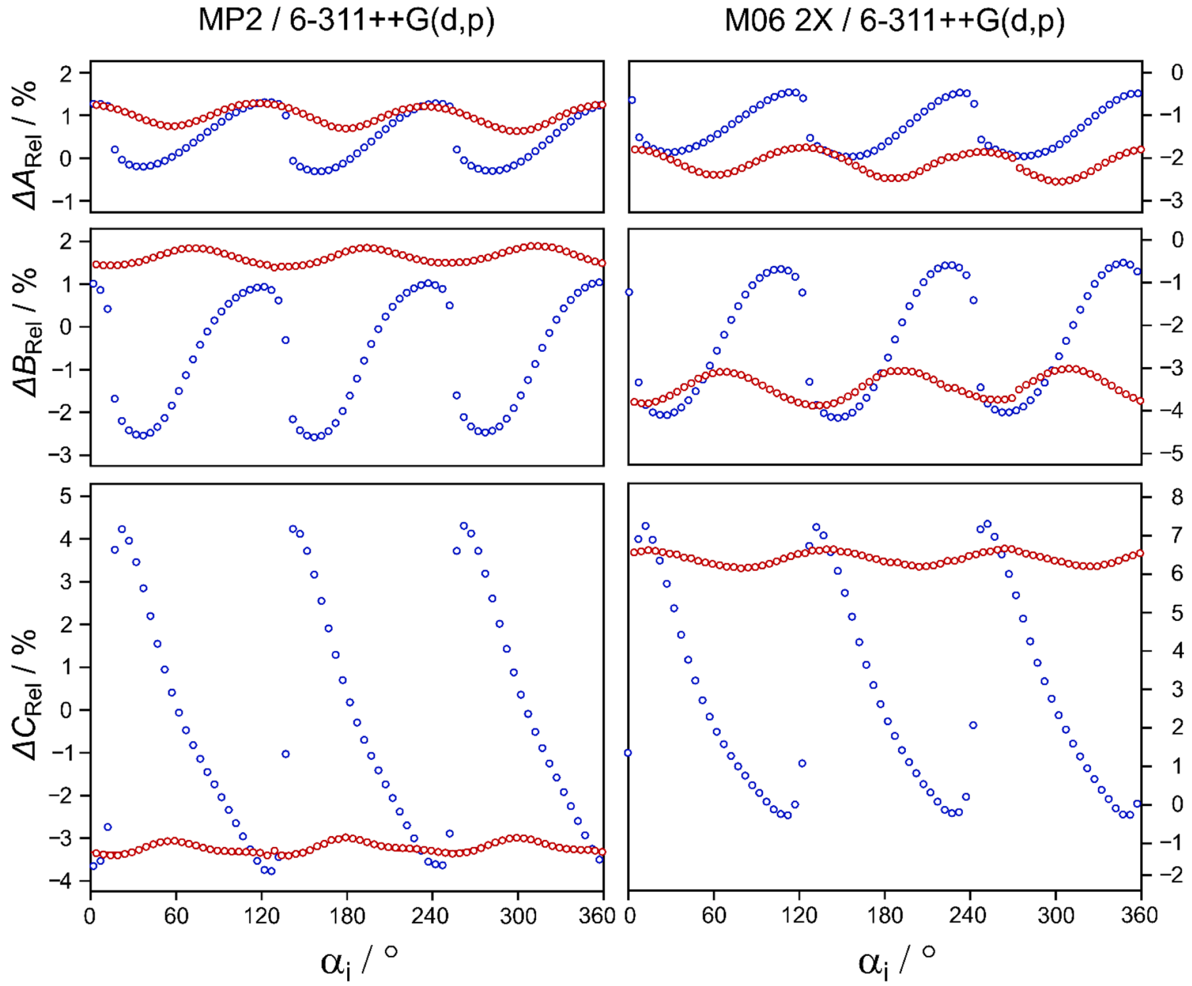

Fig. 4. Calculated modulation of the rotational constants, *A*, *B*, and *C*, during methyl internal rotation in the *t-gauche* conformer of acetic anhydride. Calculations were performed with the MP2 and M06-2X using the 6–311++G(d,p) basis set. The values are relative to the experimentally observed rotational constants. Blue represents the rotor that interacts with the remote carbonyl group (R1) and red is for the isolated methyl group (R2). α_i is for the dihedral angle of internal rotation (see Fig. 1). (For interpretation of the references to color in this figure legend, the reader is referred to the web version of this article.)

Table 3

Fitted and Computed Spectroscopic Constants for Acetic Difluoroacetic Anhydride and Comparison with Theoretical Results.

	Experimental	**M06-2X**^{a}				**MP2**^{a}		
		syn	CF_2H *t-gauche*^{90}	CH_3 *t-gauche*^{90}	CH_3 *t-gauche*^{120}	*syn*	CF_2H *t-gauche*^{90}	CH_3 *t-gauche*^{120}
A [MHz]	2910.06378(45)	2878	2930	2983	3035	2854	2872	3033
B [MHz]	1182.89553(17)	1021	1199	1009	995	1011	1195	985
C [MHz]	989.46343(13)	920	996	919	934	921	998	936
Δ_J [kHz]	0.1837(14)							
Δ_{JK} [kHz]	0.3229(70)							
Δ_K [kHz]	0.392(14)							
δ_J [kHz]	0.03318(67)							
δ_K [kHz]	–0.246(35)							
F_0 [GHz]	[158.0]^b	158.1	158.0	158.3	157.9	157.7	157.6	157.4
V_3 [cm^{-1}]	252.646(19)	305	257	248	248	315	246	272
ε [deg]	95.28(66)	18	85	18	16	19	78	9
δ [deg]	30.198(26)	58	32	70	71	57	33	70
$D_{\pi 2J}$ [MHz]	0.06020(58)							
$D_{\pi 2K}$ [MHz]	–0.3379(35)							
N^c	178							
σ [kHz]	4.0							
$\|\mu_a\|$ [D]	Strong	0.4	3.2	0.0	0.1	0.6	2.9	0.4
$\|\mu_b\|$ [D]	Weak	2.1	0.9	2.8	2.6	1.9	0.9	2.4
$\|\mu_c\|$ [D]	Weak	0.8	0.5	0.6	0.6	0.9	0.4	0.3
Rel. Energy^b.	–	1.04	0	1.89	1.89	0.00	0.36	0.95
		(0.87)		(1.83)	(1.73)		(0.47)	(0.90)

(a) All energies are in kcal/mol and were obtained using the 6–311++G(d,p) basis set. Values in parentheses are zero-point corrected. Uncorrected energies are relative to the most stable conformer calculated at the same level of theory. Zero-point corrected energies are relative to the form that has the lowest zero-point corrected energy. In cases where *t-gauche*^{90} and *t-gauche*^{120} minima are predicted, the energy given is that of the lower energy structure. Calculated rotational constants are equilibrium values.

(b) Theoretical value, constrained in fit.

(c) Number of transitions in the fit.

(Table 3). These structures are quite different and, as seen below, comparison of the observed and calculated constants given in Table 3 unambiguously establishes that the observed conformer is CF_2H *t-gauche,* i.e., the conformer in which the CF_2H hydrogen interacts with the remote carbonyl oxygen. Several other conformers were also identified but were too high in energy to be considered, and/or had calculated rotational constants whose comparison with experimental values excluded them from further consideration. The structures of all calculated conformers are provided in the Supplementary Material.

3. Experimental methods and results

Acetic anhydride and its D-6 isotopologue were purchased from Sigma-Aldrich. Acetic difluoroacetic anhydride was prepared by the reaction of acetic anhydride and difluoroacetic anhydride (commercially available) as described previously [1,16]. While the post-reaction mixtures for the other anhydrides synthesized in this manner were observed as clear, pale-yellow liquids [1], that for acetic difluoroacetic anhydride appeared as a deep mahogany colored liquid.

Spectra were taken using the dual cavity and chirped-pulse spectrometer described elsewhere [17,18]. Samples were introduced to the system by flowing argon at a pressure of ~ 0.5 atm over a 1.5 mL sample contained in a stainless-steel reservoir at room temperature. The resulting mixture of argon and anhydride vapor was then flowed through a stainless steel needle with an inner diameter of 0.016 in. directed along the axis of a jet expansion produced by pulsing argon at a stagnation pressure of ~ 1.0 atm. Spectra were initially recorded using the chirped-pulse spectrometer, and subsequent experiments on the cavity system were performed to resolve particularly dense and overlapping regions. Uncertainties in the measured frequencies were typically 10 kHz and 2 kHz for the chirped pulse and cavity spectrometers, respectively. A sample spectrum of acetic anhydride is shown in Fig. 5. Transition frequencies, assignments, and residuals from the least squares fits (described below) are provided as Supplementary Material.

3.1. Acetic anhydride

As expected, the effects of the internal rotation of two methyl rotors were apparent in the acetic anhydride spectrum, which displayed splittings arising from five distinct torsional symmetry species. The rigid rotor-like spectra arising from the AA state were readily assigned and fit using the DAPPERS package [3], and the resulting constants were then combined with predicted internal rotor parameters (V_3, δ and ε for each rotor) in the XIAM program [19]. Here, V_3 is the internal rotation barrier, and δ and ε are polar angles that are defined as follows: δ is the angle between the CH_3 top axis and the *a*-axis of the molecule, and ε is the angle between the *b*-axis of the molecule and the projection of the top axis onto the *b*-*c* plane. This procedure resulted in the assignment of some of the $K_a = 0$ and 1 transitions of the other four torsional states.

Although many transitions at this point in the analysis were still up to several hundred kHz off from their predicted frequencies, closed loops were ultimately identified and used to confidently assign over 200 transitions spread across all five torsional states (AA, EA, AE, EE, and EE*). A diagram indicating the loops identified for the AA state is shown in Fig. 6 and the analogous diagrams for the other four states are provided in the Supplementary Material. The full set of assigned transitions contains both cavity and chirped-pulse measurements and includes *a*-, *b*-, and *c*-type lines. The spectra were fit with XIAM using rotational and quartic distortion parameters as well as the V_3 methyl rotor barrier heights, the polar angles ε and δ, and the internal rotation distortion parameters $D_{\pi 2J}$, $D_{\pi 2K}$, and $D_{\pi 2-}$ [20] for each top. The addition of the top-top coupling term V_{cc} improved the predictions of the higher $K_a = 2$ and 3 transition frequencies and dropped the RMS by nearly 100 kHz, but V_{cc} was highly correlated with both V_3 parameters. Inclusion of V_6 and other additional internal rotor parameters available from XIAM$_{\text{mod}}$ [21] were attempted with no success, but restricting the fit to include only $K_a = 0$ and 1 lowered the rms residual still further. Fitted spectroscopic constants of the final fit of all assigned transitions and a fit containing only $K_a = 0$ and 1 lines for the parent species are shown in Table 1 where it may be seen that inclusion of the $K_a = 2$ and 3 lines does not significantly change any of the fitted rotational constants, barrier

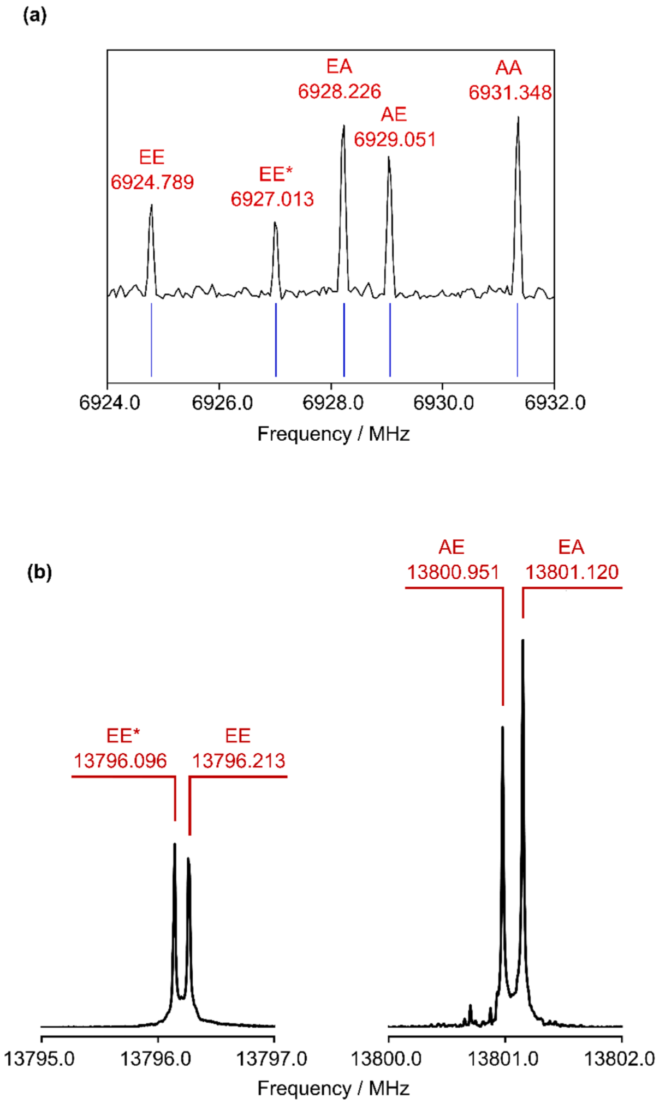

Fig. 5. (a): A portion of the chirped-pulse spectrum of acetic anhydride showing the $2_{02} \leftarrow 1_{01}$ transition. The torsional state symmetry species are indicated for the two (inequivalent) methyl internal rotors. Stick spectra are the predicted peaks. The vertical axis represents intensities in arbitrary units. **(b)**: Two high resolution spectra of the *a*-type *R*-branch $4_{04} \leftarrow 3_{03}$ transition. The torsional symmetry species are marked with the corresponding frequencies. The AA species was resolved with chirp pulse system with no further high resolution measurement required.

heights, or polar angles relative to those obtained in the $K_a = 0$, 1 only fit. Transition frequencies, assignments, and residuals from both fits are provided in the Supplementary Material. Once all the acetic anhydride spectra were assigned, the only remaining transitions in the chirped-pulse data were those of acetic acid, a known impurity in acetic anhydride.

The assignment and fitting of the D6-acetic anhydride spectrum was similar to that of the parent, except that the top-top coupling parameter and some internal rotor distortion constants were not needed to achieve an acceptable fit. Hyperfine structure resulting from the six deuterium atoms was not resolved. The parameters determined from a full fit of all assigned transitions, as well as those resulting from a fit of the K_a = 0 and 1 lines only fit are given in Table 2. As for the parent form, no significant changes in the fitted rotational constants, barrier heights, or polar angles result from the inclusion of transitions involving $K_a = 2$ and 3.

3.2. *Acetic difluoroacetic anhydride*

The assignment of the acetic difluoroacetic anhydride spectrum was more straightforward, as it contains only a single CH_3 rotor. The rigid rotor-like spectrum of the A state was assigned and fit, and the resulting constants were combined with the theoretical internal rotor parameters to produce a simulated spectrum that was highly predictive of the remaining E state transitions. The two states were then fit together with XIAM using rotational and quartic distortion parameters as well as the V_3 barrier heights, the rotor polar angles, δ and ε, and internal rotation distortion parameters. The fitted constants are given in Table 3, where differences in the relative strengths of the observed *a*-, *b*-, and *c*-type transitions are also indicated.

4. Discussion

4.1. *Acetic anhydride*

For acetic anhydride, *syn* and CH_3 *t-gauche*^{90} conformers were predicted by both the M06-2X and MP2 methods, but the CH_3 *t-gauche*^{120} conformer was also predicted with MP2 calculations. However, the relative energies of the conformers in Table 1 are all within 1 kcal/mol of each other and thus, theory does not definitively establish which is the minimum energy structure. As shown in Table 1, the rotational constants for the conformers predicted with both methods are also fairly similar, and none of the calculations stands out as giving distinctly better agreement with experiment. Thus, the calculated rotational constants do not aid in the identification of the observed form. Fortunately, however, the *syn* conformer can be ruled out on the basis of the observed transition types. Specifically, the observation of strong *a*-, *b*-, and *c*-type spectra is incompatible with the dipole moment components of the *syn* form for which $\mu_a = \mu_c = 0$ by symmetry. Moreover, as noted above, two distinct sets of internal rotation barriers were determined, which would be inconsistent with a *syn* conformer which has equivalent CH_3 rotors. The removal of the *syn* conformer from consideration leaves only the CH_3 *t-gauche*^{90} and CH_3 *t-gauche*^{120} forms, both of which are minima in the MP2 energy profile of the R1 methyl group's rotation shown in Fig. 3. Notwithstanding the possibility that one of these minima is a computational artifact or that they are both real but irrelevant to the vibrationally averaged structure, the predicted constants and polar angles of both *t-gauche* conformers are generally in moderate agreement with the fitted values. Moreover, a comparison of the fitted and predicted constants of the D6-acetic anhydride is shown in Table 2, and the results parallel those of the parent: poor agreement with the *syn* conformer and generally reasonable agreement with at least one of the *t-gauche* forms. Therefore, we conclude that acetic anhydride was observed in a *t-gauche* configuration, though it cannot be established whether a CH_3 *t-gauche*^{90} or CH_3 *t-gauche*^{120} conformer was observed or whether these are even distinct species.

Agreement between experimental and calculated rotational constants for the *t-gauche* species ranges from 0.1 % to 6.5 %, with the largest error associated with the *C* constant. While this level of discrepancy is not enough to refute the assignment to a *t-gauche* form, we note that it is somewhat worse than what has been observed for other anhydrides previously studied in the *syn* configuration [1–3]. For those systems, using the same levels of theory as applied in this work, agreement between observed and calculated values was typically within about 1 %. While it is unclear why the same levels of theory do not perform as well in the present case, a number of factors could contribute. For example, the significant variation in the rotational constants along the R1 internal rotation coordinate that result from flexing of the molecular frame (Fig. 4) likely compound the normally expected differences between equilibrium and vibrationally averaged constants. Contamination of the fitted rotational constants from untreated Coriolis interactions arising from the low frequency flexing motion could also be a contributing factor.

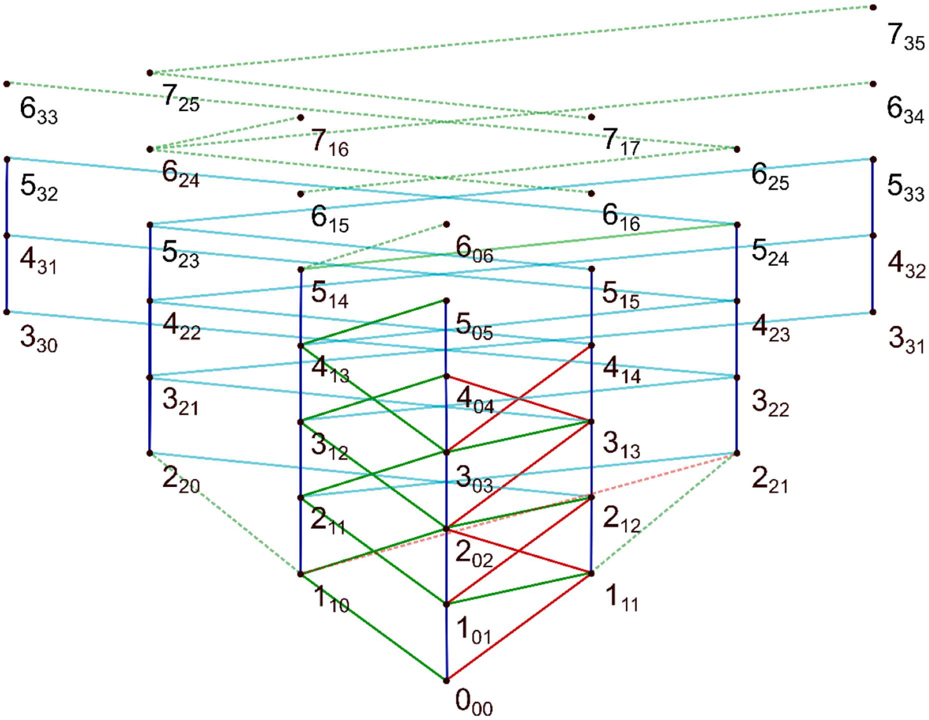

Fig. 6. Energy diagram depicting the closed loops used to assign the AA torsional state of acetic anhydride. The color coding highlights closed loops with similar transitions which differ only by *J*. Dashed lines denote additional observed transitions. Analogous diagrams for the other torsional states are provided in the Supplementary Material.

Values of V_3^{R1} and V_3^{R2} are returned by the XIAM fit, but the fit does not identify which barrier height corresponds to which rotor. However, the observed and predicted values of δ (the polar angle between the rotor axis and the *a*-axis of the molecule) do distinctly favor the labeling given in Fig. 2. (Values of ε are less conclusive, but not inconsistent.) This assignment also generally preserves the ordering of the V_3 barriers, with $V_3^{R1} > V_3^{R2}$ determined both experimentally and computationally. (The only exception is the MP2 values for the CH_3 *t-gauche*^{90} configuration for which V_3^{R1} and V_3^{R2} are calculated to be 194 and 222 cm^{-1}, respectively.) The calculated values of the barriers for the *t-gauche* forms are only in modest agreement with the fitted value, with levels of agreement ranging from 5 % to 50 %, depending on the method of calculation. This level of agreement is, again, somewhat worse than that observed for several of the anhydrides previously reported in the *syn* configuration, for which computed and fitted barrier heights differed in the 1–11 % range. Two factors likely contribute to this. The first is that the irregularity in the energy profiles shown in Fig. 3 is not well represented by the simple cosine function used in XIAM (or virtually any other treatment of internal rotation). The second is that the inclusion of the top-top coupling term, V_{cc}, which was used to lower the rms deviation in the fits, gave rise to significant correlation between the fitted V_3 values. In this regard, it is significant that the fitted barriers for D6-acetic anhydride, which did not require the inclusion of a V_{cc} term, are notably different from those of the parent and are in better agreement with the computational results (at least for the MP2 method). Thus, the fitted values for the deuterated form may be more reliable than those for the parent. Note that the fitted centrifugal distortion constants of acetic anhydride are much larger than those of acetic difluoroacetic anhydride and other anhydrides previously reported [1–3]. Thus, it seems likely that they are effective constants that are absorbing inaccuracies in the treatment of the internal rotation. It is also interesting to note that the recently assigned microwave spectrum of 4,5–dimethylthiazole [22] bears some striking similarities in that it, too, includes two coupled methyl rotors with poorly predicted V_3 barriers and an XIAM fit with a V_{cc} term highly correlated to the V_3 parameters.

4.2. Acetic difluoroacetic anhydride

For acetic difluoroacetic anhydride, a CF_2H *t-gauche*^{90} conformer is predicted in addition to the *syn*, CH_3 *t-gauche*^{90}, and CH_3 *t-gauche*^{120} forms (as well as a few other that were excluded from consideration for reasons discussed above). Comparison between the observed and calculated rotational constants, internal rotation barrier, methyl group polar angles, and *a*-, *b*, and *c*-type intensities all strongly support the assignment of the observed species to a CF_2H *t-gauche* conformer. Moreover, the M06-2X calculations predict this to be the lowest energy form, though we note that the MP2 calculations place it slightly higher in energy (~0.4 kcal) than the *syn* conformer (which, again, is a computationally insignificant amount). The M06-2X and MP2 calculations differ in that the former predict the global minimum energy configuration to be CF_2H *t-gauche*^{90} while the latter predict it to be *syn*. However, the preference for the *syn* conformer returned by the MP2 calculations is marginal, (0.36 kcal/mol) and within the expected computational error. The preference for the CH_2F *t-gauche*^{90} structure obtained at the M06-2X level is somewhat more decisive (1.0 kcal/mol), but still pushing the limits to which these levels of theory are expected to be reliable. In the CF_2H *t-gauche*^{90} conformer, the hydrogen bonded alpha hydrogen is that of the difluoromethyl group rather than that of the methyl group. *T-gauche*^{90} and *t-gauche*^{120} structures involving a CH_3 hydrogen were also identified, but are of significantly higher energy than the CF_2H *t-gauche*^{90} structure, presumably due to the reduced acidity of the methyl hydrogens the relative to that of the CF_2H group. Indeed, experimental and theoretical work has indicated the ability of the CF_2H group to serve as a hydrogen bond donor [23,24].

5. Conclusion

Supersonic jet microwave spectra of acetic anhydride and acetic difluoroacetic anhydride have been observed and analyzed. The results establish that both systems were observed in a nonplanar *t-gauche* conformation. This is in contrast to other anhydrides studied which have been shown to adopt either a *syn* or *planar trans* configuration. While M06-2X and MP2 calculations using a 6-311++G(d,p) basis set predict both *syn* and *t-gauche* forms, the energy ordering is within the expected accuracy of the calculations. Thus, the calculations do not definitively establish the lowest energy conformation. The low temperature of the supersonic jet, however, presumably freezes the system into its lowest energy form, and the observation of *t-gauche* conformers strongly suggests that they correspond to the lowest energy structure for each system. The preference for a *t-gauche* conformation over a *syn* conformation appears to arise from a non-covalent interaction between a hydrogen of the CH_3 group (in acetic anhydride) or the hydrogen of the CF_2H group (in acetic difluoroacetic anhydride) with the oxygen of the carbonyl group to which it is not directly bonded. This gives rise to a six-membered ring structure in both cases. For acetic anhydride, calculations indicate that the molecular frame flexes significantly as the CH_3 group in the ring rotates and, moreover, indicates a switching of the non-covalently interacting hydrogen as the CH_3 proceeds along its internal rotation coordinate. This produces an irregular potential energy profile and likely contributes to larger discrepancies between theoretical and experimental constants than have been observed for related anhydrides at the same levels of theory.

CRediT authorship contribution statement

Nathan Love: Writing – original draft, Validation, Investigation, Formal analysis, Data curation, Conceptualization. **Kenneth J. Koziol:** Writing – review & editing, Validation, Formal analysis. **Kaitlyn Belmont:** Formal analysis. **Kenneth R. Leopold:** Writing – review & editing, Validation, Supervision, Resources, Project administration, Funding acquisition, Conceptualization.

Declaration of competing interest

The authors declare that they have no known competing financial interests or personal relationships that could have appeared to influence the work reported in this paper.

Data availability

Data will be made available on request.

Acknowledgements

This work was supported by the National Science Foundation (Grant No. CHE 1953528) and the Minnesota Supercomputing Institute. We thank Professor Jason Goodpaster for suggesting and performing the CCSD calculations and Professor Tom Hoye for helpful discussions about stereochemistry.

Appendix A. Supplementary data

Cartesian coordinates for calculated structures; results of DLPNO-CCSD(T)/aug-cc-pvtz and DLPNO-CCSD(T)/aug-cc-pvqz calculations; observed transition frequencies, assignments, and residuals from the least squares fits; closed loops for the AE, EA, EE and EE* torsional states of acetic anhydride; structures of all potential minima located for acetic difluoroacetic anhydride; video showing the flexing of the molecular frame as the ring-forming CH_3 group in acetic anhydride internally rotates. Supplementary data to this article can be found online at https://doi.org/10.1016/j.jms.2024.111926.

References

[1] N. Love, A.J. Reynolds, M.A. Dvorak, K.R. Leopold, Conformational analysis of carboxylic anhydrides: a microwave and computational study, J. Mol. Spectrosc. 397 (2023) 111844.

[2] N. Love, C.J. Smith, A.K. Huff, K.R. Leopold, A microwave and computational study of trifluoroacetic anhydride, J. Mol. Spectrosc. 365 (2019) 111210.

[3] N. Love, A.K. Huff, K.R. Leopold, A new program for the assignment and fitting of dense rotational spectra based on spectral progressions: application to the microwave spectrum of pivalic anhydride, J. Mol. Spectrosc. 370 (2020) 111294.

[4] A. Boogaard, H.J. Geise, F.C. Mijlhoff, An electron diffraction investigation of the molecular structure of formic anhydride, J. Mol. Struct. 13 (1972) 53–58.

[5] G. Wu, S. Shlykov, C. Van Alsenoy, H.J. Geise, E. Sluyts, B.J. Van der Veken, Formic anhydride in the gas phase, studied by electron diffraction and microwave and infrared spectroscopy, supplemented with ab-initio calculations of geometries and force fields, J. Phys. Chem. 99 (1995) 8589–8598.

[6] S. Vaccani, A. Bauder, Hs. H. Günthard, Microwave spectrum, dipole moment and conformation of formic anhydride, Chem. Phys. Lett. 35 (1975) 457–460.

[7] S. Vaccani, U. Roos, A. Bauder, Hs H. Günthard, Microwave spectra, substitution structure and vibrational satellites of formic anhydride, Chem. Phys. 19 (1977) 51–57.

[8] H.J. Vledder, F.C. Mijlhoff, F.P. Van Well, G.M.T. Dofferhoff, J.C. Leyte, An electron diffraction investigation of the molecular structure of formic acetic anhydride, J. Mol. Struct. 9 (1971) 25–32.

[9] G. Wu, S. Shlykov, C. Van Alsenoy, H.J. Geise, E. Sluyts, B.J. Van der Veken, Formic acetic anhydride in the gas phase, studied by electron diffraction and infrared spectroscopy, supplemented with ab-initio calculations of geometries and force fields, J. Phys. Chem. 100 (1996) 11620–11629.

[10] A. Bauder, Microwave spectrum of formic acetic anhydride, Mol. Phys. 111 (2013) 1999–2002.

[11] H.J. Vledder, F.C. Mijlhoff, J.C. Leyte, Vibrational structure and normal coordinate analysis of formic acetic anhydride, J. Mol. Struct. 10 (1971) 57–73.

[12] G. Wu, C. Van Alsenoy, H.J. Geise, E. Sluyts, B.J. Van der Veken, I.F. Shishkov, L. V. Khristenko, Acetic anhydride in the gas phase, studied by electron diffraction and infrared spectroscopy, supplemented with ab initio calculations of geometries and force fields, J. Phys. Chem. 104 (2000) 1576–1587.

[13] H.J. Vledder, F.S.M. Van Kleef, F.C. Mijlhoff, J.C. Leyte, Vibrational spectra, normal coordinate analysis, and conformation of acetic anhydride, J. Mol. Struct. 10 (1971) 189–202.

[14] H.J. Vledder, F.C. Mijlhoff, J.C. Leyte, C. Romers, An electron diffraction investigation of the molecular structure of gaseous acetic anhydride, J. Mol. Struct. 7 (1971) 421–429.

[15] Gaussian 16, Revision C.01, M.J. Frisch, G.W. Trucks, H.B. Schlegel, G.E. Scuseria, M.A. Robb, J.R. Cheeseman, G. Scalmani, V. Barone, G.A. Petersson, H. Nakatsuji, X. Li, M. Caricato, et al., Gaussian, Inc., Wallingford CT (2016).

[16] E.J. Bourne, M. Stacey, J.C. Tatlow, R. Worrall, Studies of Trifluoroacetic Acid. Part XII. Acyl Trifluoroacetates and Their Reactions, J. Chem. Soc. 2006–2012 (1954).

[17] J.A. Phillips, M. Canagaratna, H. Goodfriend, A. Grushow, J. Almlöf, K.R. Leopold, Microwave and ab Initio investigation of $HF\text{-}BF_3$, J. Am. Chem. Soc. 117 (1995) 12549–12556.

[18] C.T. Dewberry, R.B. Mackenzie, S. Green, K.R. Leopold, 3D-printed slit nozzles for fourier transform microwave spectroscopy, Rev. Sci. Instrum. 86 (2015) 065107.

[19] H. Hartwig, H. Dreizler, The microwave spectrum of trans-2,3-dimethyloxirane in torsional excited states, Z. Naturforsch. 51a (1996) 923–932.

[20] L. Ferres, W. Stahl, H.V.L. Nguyen, Conformational effects on the torsional barriers in m-methylanisole studied by microwave spectroscopy, J. Chem. Phys. 148 (2018) 124304.

[21] S. Herbers, H.V.L. Nguyen, Next level of achievement of the XIAM code in modeling the microwave spectra of m-methylanisole, J. Mol. Spectrosc. 370 (2020) 111289.

[22] V. Van, T. Nguyen, W. Stahl, H.V.L. Nguyen, I. Kleiner, Coupled large amplitude motions: the effects of two methyl internal rotations and ^{14}N quadrupole coupling in 4,5-dimethylthiazole investigated by microwave spectroscopy, J. Mol. Struct. 1207 (2020) 127787.

[23] J.A. Erickson, J.I. McLoughlin, Hydrogen bond donor properties of the difluoromethyl group, J. Org. Chem. 60 (1995) 1626–1631.

[24] C.D. Sessler, M. Rahm, S. Becker, J. Goldberg, R. Wang, S.J. Lippard, CF_2H, a hydrogen bond donor, J. Am. Chem. Soc. 139 (2017) 9325–9332.